Asian Journal of
Science, Technology, Engineering, and Art

e-ISSN: 3025-4507
p-ISSN: 3025-5287
Index: Harvard, Boston, Sydney University, Dimensions, Lens, Scilit, Semantic, Google, etc

https://doi.org/10.58578/AJSTEA.v3i1.4841

Dynamic Models of the Infection of Lassa Fever Epidemics Incorporating Detected and Undetected Class

Hamisu Idi[1], Kazeem E. Lasisi[2], M. Abdulhameed[3], A.M. Kwami[4], Muhammad Mubarak Muhammad[5]
[1,5]Federal Polytechnic, Bauchi, Nigeria
[2,3,4]Abubakar Tafawa Balewa University, Bauchi, Nigeria
ahidi@fptb.edu.ng; bkazeemlasisi@gmail.com

Article Info:

Submitted:	Revised:	Accepted:	Published:
Dec 1, 2024	Dec 18, 2024	Jan 27, 2025	Feb 1, 2025

Abstract

In the scope of this research endeavor, we embarked on the development of a dynamic model, intricately designed to scrutinize the intricate dynamics of Lassa fever transmission, encompassing both detected and undetected cases. Our central objective revolved around the meticulous examination of how a vaccine could exert its influence on the transmission dynamics of Lassa disease. The study encompassed an exhaustive exploration of the model's equilibrium states, diligently scrutinizing both disease-free and endemic equilibria. To shed light on the potential for disease spread, we calculated the pivotal epidemiological parameter, the basic reproduction number, employing the rigorous next-generation matrix methodology. Subsequently, we delved into a comprehensive stability analysis, encompassing both local and global stability assessments. The Routh-Hurwitz conditions were harnessed for local stability analysis, while the Castillo-Chavez criterion was leveraged for global stability analysis. In our quest for a profound understanding, we ventured into analytical techniques to derive exact solutions for the model, coupled with numerical computations facilitated by the versatile MATHEMATICA

AJSTEA Journal is licensed under a Creative Commons Attribution-NonCommercial-ShareAlike 4.0 International License

software. The culmination of our endeavors unveiled a compelling insight: the disease-free equilibrium attains local asymptotic stability if and only if the basic reproduction number assumes a value below unity; conversely, it stands as unstable when this threshold is exceeded. In essence, this implies that the complete eradication of Lassa fever is within reach when the secondary infection rate remains constrained below a critical threshold.

Keywords: Lassa Fever, Vaccine, Basic Reproduction Number

INTRODUCTION

Lassa fever, alternatively recognized as Lassa hemorrhagic fever (LHF), emerges as an acute viral hemorrhagic ailment originating from the Lassa virus (LASV). Its symptomatic manifestation within humans spans a duration of 2 to 21 days, and it recurrently ushers in outbreaks within the Western African region [1]. LASV's endemicity blankets extensive swathes of sub-Saharan West Africa, underscored by recurrent and widespread outbreaks [2]. Noteworthy are the high-risk zones for LHF, encapsulating roughly 80% of Sierra Leone and Liberia, 50% of Guinea, 40% of Nigeria, along with substantial segments of Benin, Cote d'Ivoire, Togo, and Ghana [3, 4]. The year 2018 bore witness to an exceptionally pronounced surge in Lassa fever cases within Nigeria, prompting the World Health Organization (WHO) to designate it as an outbreak of considerable magnitude, characterized as a grade 2 public health emergency [5]. The Nigerian Center for Disease Control (NCDC) documented a total of 431 laboratory-confirmed cases, inclusive of 37 healthcare personnel, dispersed across 21 states in 2018, with an estimated case fatality rate of 25% [6]. Nigeria has consistently borne the predominant burden of reported cases, notably so in 2019 and 2020.

The transmission of LASV primarily occurs through direct exposure to rat urine, feces, saliva, or materials contaminated with these substances. In specific regions, the practice of consuming rodents as a food source further heightens the risk of exposure [7]. Additionally, LASV can be transmitted among humans through direct contact with infected bodily fluids such as blood, urine, and feces [3]. Epidemiological modeling studies have indicated that 20% of hospitalized Lassa fever cases result from human-to-human transmission, with certain individuals acting as particularly efficient spreaders [8].

Current strategies aimed at preventing LASV infection predominantly involve avoiding both direct and indirect contact with secretions and excretions from the Mastomys rodent. Enhanced hygiene practices in healthcare facilities are also crucial components of these strategies [9]. However, the effective implementation of these measures has presented challenges, and they are unlikely to achieve comprehensive control in the foreseeable future [10]. Promising studies support the development of a LASV vaccine, although these vaccine candidates have not yet undergone clinical trials [11, 12].

The utilization of mathematical modeling studies proves invaluable for assessing the potential impact of a LASV vaccine in endemic regions, enabling the optimization of resource allocation in a context where resources are limited. Various mathematical models have been developed for LASV, some of which subdivide the rodent population, consider human immigration, and calculate the basic reproductive number. These models have assessed disease spread and control, stability, sensitivity of parameters, and the effects of control measures on different model compartments. Recent models have suggested strategies such as continuous control or rodent vaccinations, the use of multiple intervention strategies, and the potential for disease elimination under certain conditions. The incorporation of vaccination, rodents-to-humans and human-to-human transmissions, seasonality, and immunity has also been explored, indicating that vaccination in endemic areas could significantly reduce disease incidence. However, existing models primarily focus on continuous or pulse vaccination and do not include detected or non-detected compartments.

In light of the aforementioned literature, this study seeks to enhance existing models by proposing mathematical models that incorporate both detected and non-detected compartments. The objective of this approach is to offer a more thorough comprehension of the dynamics related to the transmission and control of Lassa fever in Nigeria.

Model Formulation

Mode diagram

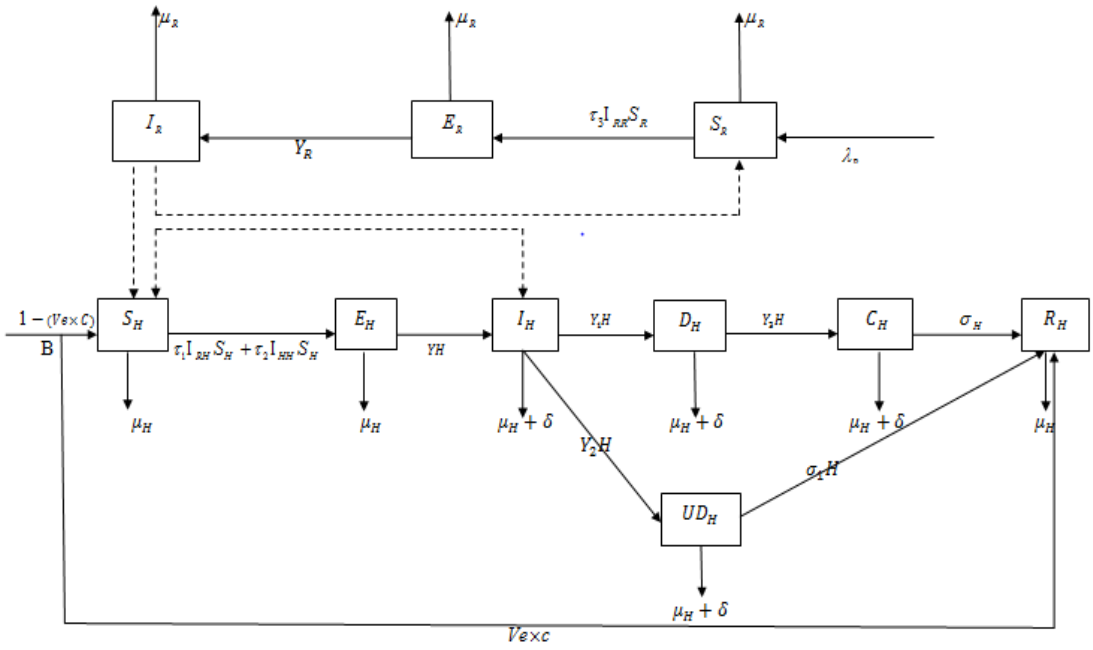


Fig. 1, Schematic diagram of Lassa fever model with pulse vaccination

The susceptible human population increases at a specified rate due to the birth of new individuals and the decline in immunity resulting from vaccination, with 'v' denoting vaccine effectiveness and 'c' representing vaccination coverage. Conversely, this population decreases due to fresh infections occurring from interactions between infected humans or rodents and the susceptible population at particular rates 'β' and 'α', respectively. Furthermore, natural deaths contribute to the reduction of this population at a fixed rate 'μ'.

The exposed human population increases because newly infected individuals migrate from the susceptible group at a rate 'β,' and it decreases due to individuals transitioning from this category to the infected class at a rate 'σ'. Natural deaths also contribute to the reduction of this population at a rate 'μ'.

The infected human population, denoted as IH, increases due to individuals moving from the exposed class at a rate 'δ' and decreases as infected individuals migrate to detected and undetected compartments at rates 'ϕ' and 'ψ,' respectively. Furthermore, this population

declines due to both natural deaths and deaths caused by the disease at rates 'μ' and 'γ', respectively.

The population of identified individuals expands as individuals migrate from the infected group at a rate of 'ϕ', but it contracts as individuals transition to the isolation category at a rate of 'λ'. This change is further influenced by both natural and disease-induced fatalities, transpiring at rates 'μ' and 'θ', respectively.

The undetected population experiences growth as individuals move from the infected group at a rate labeled as 'ϕ'. Conversely, it declines as these individuals migrate into the recovered human population at a rate 'λ'. Furthermore, this population dwindles due to natural fatalities at a rate of 'μ' and fatalities resulting from the disease at a rate of 'γ'.

Model Equation

$$\frac{\partial S_H}{\partial t} = B\left[1-(Ve\times c)\right]-(\tau_1 \mathrm{I}_{RH}+\tau_2 \mathrm{I}_{HH})S_H-\mu_H S_H$$

$$\frac{\partial E_H}{\partial t} = (\tau_1 \mathrm{I}_{RH}+\tau_2 \mathrm{I}_{HH})S_H-(\mu_H+\mathrm{Y}_H)E_H$$

$$\frac{\partial \mathrm{I}_H}{\partial t} = \mathrm{Y}_H E_H-(Y_{1H}+Y_{2H}+\mu_H+\delta)\mathrm{I}_H$$

$$\frac{\partial D_H}{\partial t} = Y_{1H}\mathrm{I}_H-(Y_{3H}+\mu_H+\delta)D_H)$$

(1)

$$\frac{\partial UD_H}{\partial t} = Y_{2H}\mathrm{I}_H-(\sigma_{1H}+\mu_H+\delta)UD_H$$

$$\frac{\partial R_H}{\partial t} = \sigma_H C_H+\sigma_{1H}UD_H+B(Ve\times c)-\mu_H R_H$$

$$\frac{\partial S_R}{\partial t} = \lambda_R-\tau_3 \mathrm{I}_{RR}S_R-\mu_R S_R$$

$$\frac{\partial E_R}{\partial t} = \tau_3 \mathrm{I}_R S_R-(\mathrm{Y}_R+\mu_R)E_R$$

$$\frac{\partial \mathrm{I}_R}{\partial t} = \mathrm{Y}_R E_R - \mu_R \mathrm{I}_R$$

Where $N_H = S_H + E_H + I_H + D_H + UD_H + C_H + R_H$

And $N_R = S_R + E_R + I_R$

Basic properties of the deterministic model

We present the following result for the analysis of our model (1)

Positivity of the Solution

It is very imperative to ensure that all the solutions of the deterministic equations always remain non – negative so long as the initial values are non – negative. In order to proof this, the following theorem will be use:

Theorem (1): Assuming non-negative initial state values for model (1) , $S_H \geq 0$,

$$E_H \geq 0,\ \mathrm{I}_H \geq 0,\ D_H \geq 0,\ UD_H \geq 0,\ C_H \geq 0,\ R_H \geq 0,\ S_R \geq 0,\ E_R \geq 0,\ I_R \geq 0$$

,

Then all solutions remain non – negative for t > 0.

Proof:-

$$\frac{dS_H}{dt} = B\left[1-(ve\times c)\right] - (\tau_1 \mathrm{I}_{RH} + \tau_2 \mathrm{I}_{HH})S_H - \mu_H S_H$$

$$\frac{dS_H}{dt} \geq -(\tau_1 \mathrm{I}_{RH} + \tau_2 \mathrm{I}_{HH})S_H - \mu_H S_H$$

$$\frac{dS_H}{dt} \geq -(\tau_1 \mathrm{I}_{RH} + \tau_2 \mathrm{I}_{HH} + \mu_H)dt$$

Integrating both sides we get

$$\left|\ln S_H\right| \geq -(\tau_1 \mathrm{I}_{RH} + \tau_2 \mathrm{I}_{HH} + \mu_H)t + C$$

$$S_H(t) \geq Ae^{-(\tau_1 \mathrm{I}_{RH} + \tau_2 \mathrm{I}_{HH} + \mu_H)t}$$

Where $A = e^C$

$S_H(t) \geq Ae^{-(\tau_1 I_{RH} + \tau_2 I_{HH} + \mu_H)t}$ (2) Applying the initial condition $t = 0$

$$S_H(0) \geq Ae^0 \Rightarrow A \leq S_H(0)$$

Substituting back into equation (2)

$$S_H(t) \geq S_H(0)e^{-(\tau_1 I_{HR} + \tau_2 I_{HH} + \mu_H)t} \geq 0 \quad (3)$$

Similarly, we can readily demonstrate that all solutions of models (1) will stay positive if the initial values are positive.

Boundedness

We must also ensure that, our model (1) does not grows unboundedly since usually population are mostly limited in their growth due to certain factors such as death, carrying capacity of the environment, competition, migration, etc. therefore, we would study the boundedness of model (1) as follows:

$$\frac{dN_H}{dt} = \frac{d}{dt}(S_H + E_H + I_H + D_H + UD_H + C_H + R_H)$$

And

$$\frac{dN_R}{dt} = \frac{d}{dt}(S_R + E_R + I_R)$$

So that by solving we get

$$N_H(t) \leq \frac{B}{\mu_H} - (B - \mu_H N_H(0))e^{-\mu t} \quad (4)$$

and

$$N_R(t) \le \frac{\lambda_R}{\mu_R} - \frac{(\lambda_R - \mu_R N_R(0))\ell^{-\mu}}{\mu_R} \quad (5)$$

As $t->\infty$ in (4) and (5) the population size $N_H \to \frac{B}{\mu_H}$ which means that $0 \le N_H \le \frac{B}{\mu_H}$, and the population size $N_R \to \frac{\lambda_R}{\mu_R}$, which means that $0 \le N_R \le \frac{\lambda_R}{\mu_R}$. Thus, the system (1) is bounded in the region Ω_1 and Ω_2. Where

$$\Omega_1 = \left\{ S_H, E_H, I_H, D_H, UD_H, C_H, R_H, \in R^T{}_+ : S_H + E_H + I_H + D_H + UD_H + C_H + R_H \le \frac{B}{\mu_H} \right\} \text{and}$$

$$\Omega_2 = \left\{ S_R, E_R, \mathrm{I}_R, \in R^I{}_+ \ : S_R + E_R + \mathrm{I}_R \le \frac{\lambda_R}{\mu_R} \right\}$$

It is therefore, biologically feasible to study the system (1) in the region Ω_1 and Ω_2 because it is mathematically well posed and positively invariant.

Lassa-free equilibrium

In the absence of Lassa fever, the susceptible population undergoes changes in proportion based on their recruitment rates (births) relative to their death rate, as indicated by equation (6).

$$(S_H, E_H, \mathrm{I}_H, D_H, UD_H, C_H, R_H, S_R, E_R, I_R) = (\frac{B}{\mu_H}, 0, 0, 0, 0, 0, 0, \frac{\lambda_R}{\mu_R}, 0, 0) \quad (6)$$

It indicate that in the absence of Lassa fever, the susceptible population undergoes changes in proportion based on their recruitment rates (births) relative to their death rate.

3.4 Endemic Equilibrium

To compute the endemic equilibrium point, it is essential to illustrate that $E_H \neq 0$, $I_H \neq 0$, $D_H \neq 0$, $UD_H \neq 0$, $C_H \neq 0$, $E_R \neq 0$, and $I_R \neq 0$.

$$D_H \neq 0, UD_H \neq 0, C_H \neq 0, E_R \neq 0, \text{and } I_R \neq 0.$$

$$\left.\begin{aligned}
S^{**}_H &= \frac{B(1-(Ve\times c)}{\mu^2_R K_1(\tau_1 \Upsilon_R \lambda_R K_1+\tau_2 \Upsilon_H)B(1-(Ve\times c)(\Upsilon_R+\mu_R)} \\
E^{**}_H &= \frac{B\left[1-(Ve\times c)\right]}{(\mu_H)(\mu_H+\Upsilon_H)} \\
I^{**}_H &= \frac{\Upsilon_H(B(1-(Ve\times c))}{(\mu_H)(\mu_H+\Upsilon_H)Y_{1H}+Y_{2H}+\mu_H+\delta} \\
D^{**}_H &= \frac{Y_{1H}\Upsilon_H B(1-(Ve\times c))}{(\mu_H)(\mu_H+\Upsilon_H)(Y_{1H}+Y_{2H}+\mu_H+\delta)(Y_{3H}+\mu_H+\delta)} \\
UD^{**}_H &= \frac{Y_{2H}\Upsilon_H B(1-(Ve\times c))}{(\mu_H)(\mu_H+\Upsilon_H)(Y_{1H}+Y_{2H}+\mu_H+\delta)(\sigma_{1H}+\mu_H+\delta)} \\
C^{**}_H &= \frac{Y_{3H}Y_{1H}\Upsilon_H B(1-(Ve\times c)}{(\mu_H)(\mu_H+\Upsilon_H)(Y_{1H}+Y_{2H}+\mu_H+\delta)(Y_{3H}+\mu_H+\delta)(\sigma_H+\mu_H+\delta)} \\
R^{**}_H &= \frac{\Upsilon_H B(\sigma_H \Upsilon_{3H}\Upsilon_{1H}(1-(Ve\times C)(\sigma_{1H}+\mu_H+\delta)+\sigma_{1H}\Upsilon_{2H}\Upsilon_H(\Upsilon_{3H}+\mu_H+\delta)(\sigma_H+\mu_H+\delta)}{\mu^2_H(\Upsilon_H+\mu_H)(\Upsilon_{1H}+\Upsilon_{2H}+\mu_H+\delta)(\Upsilon_{3H}+\mu_H+\delta)(\sigma_H+\mu_H+\delta)(\sigma_{1H}+\mu_H+\delta)} \\
S^{**}_R &= \frac{\lambda_R}{(\tau_3 \Upsilon_R \lambda_R+\mu_R)(\Upsilon_R+\mu_R)\mu^2_R} \\
I^{**}_R &= \frac{\Upsilon_R \lambda_R}{\mu^2_H(\Upsilon_R+\mu_R)} \\
E^{**}_R &= \frac{\lambda_R}{\mu_R(\Upsilon_R+\mu_R)}
\end{aligned}\right\} \quad (7)$$

This implies that, the disease will continue to be endemic in the population.

Basic Reproduction Number

The fundamental reproduction number, commonly symbolized as R_0 (pronounced as "R naught"), signifies the average count of secondary infections generated by each infectious individual throughout their period of infectivity. It stands as a pivotal epidemiological metric employed to gauge the potential for disease transmission within a population. If R_0 surpasses 1, it signifies the likelihood of an infectious disease spreading within the population, whereas if it falls below 1, the disease is anticipated to diminish over time. R_0 plays a crucial role in enabling researchers and public health authorities to comprehend the contagiousness and potential consequences of an infectious disease outbreak. Thus, $G = FV^{-1}$

$$FV^{-1}=\begin{pmatrix} 0 & \frac{\tau_2 B}{\mu_H} & 0 & 0 & 0 & 0 & \frac{\tau_1\lambda_R}{\mu_R} \\ \mathrm{Y}_H & 0 & 0 & 0 & 0 & 0 & 0 \\ 0 & \mathrm{Y}_{1H} & 0 & 0 & 0 & 0 & 0 \\ 0 & \mathrm{Y}_{2H} & 0 & 0 & 0 & 0 & 0 \\ 0 & 0 & \mathrm{Y}_{1H} & 0 & 0 & 0 & 0 \\ 0 & 0 & 0 & 0 & 0 & 0 & \frac{\tau_3\lambda_R}{\mu_R} \\ 0 & 0 & 0 & 0 & 0 & \mathrm{Y}_R & 0 \end{pmatrix} \begin{pmatrix} \frac{1}{r_1} & 0 & 0 & 0 & 0 & 0 & 0 \\ 0 & \frac{1}{r_2} & 0 & 0 & 0 & 0 & 0 \\ 0 & 0 & \frac{1}{r_3} & 0 & 0 & 0 & 0 \\ 0 & 0 & 0 & \frac{1}{r_4} & 0 & 0 & 0 \\ 0 & 0 & 0 & 0 & \frac{1}{r_5} & 0 & 0 \\ 0 & 0 & 0 & 0 & 0 & \frac{1}{r_6} & 0 \\ 0 & 0 & 0 & 0 & 0 & 0 & \frac{1}{r_7} \end{pmatrix} \quad (8)$$

Therefore, we solved for the lambda $\left|FV^{-1}-\lambda 1\right|=0$ and obtained the eigenvalues $R_{0,H}$ and $R_{0,R}$ as follow

$$R_{0,R}=\lambda_4=\frac{\mu_R\sqrt{(\mathrm{Y}_R+\mu_R)\mathrm{Y}_R\tau_1\lambda_R}}{(\mu_R)^2(\mathrm{Y}_R+\mu_R)}, \qquad R_{0,H}=\frac{\sqrt{\mu_H(\mathrm{Y}_H+\mu_H)(\mathrm{Y}_{1H}+\mathrm{Y}_{2H}+\mu_H+\delta)\mathrm{Y}_H\tau_2 B}}{\mu_H(\mathrm{Y}_H+\mu_H)(\mathrm{Y}_{1H}+\mathrm{Y}_{2H}+\mu_H+\delta)}$$

And the threshold $R_{0,(H,R)}$ which is the secondary infection that can be generated by any infectious person during his/her lifetime as an infectious person. When the value of $R_{0,(H,R)}<1$ the disease will dies out and if $R_{0,(H,R)}>1$ the Lassa fever disease will continue to spread and become endemic in the population.

$$R_{0,(H,R)}=\frac{\sqrt{\mathrm{Y}_R(\mathrm{Y}_R+\mu_R)\tau_1\lambda_R+\mu_H(\mathrm{Y}_H+\mu_H)(\mathrm{Y}_{1H}+\mathrm{Y}_{2H}+\mu_H+\delta)\mathrm{Y}_H\tau_2 B}}{\mu_H(\mathrm{Y}_H+\mu_H)(\mathrm{Y}_{1H}+\mathrm{Y}_{2H}+\mu_H+\delta)(\mathrm{Y}_R+\mu_R)\mu_R} \quad (9)$$

Examining the Disease-Free Equilibrium

Theorem (2) states that the disease-free equilibrium is locally asymptotically stable if $R_0<1$

Proof:

The Jacobian matrix at the disease-free equilibrium is derived as follows:

$$J_{E0} == \begin{pmatrix} -\mu_H & 0 & \frac{-\tau_2 B}{\mu_H} & 0 & 0 & 0 & 0 & 0 & 0 & -\frac{\tau_1 \lambda_R}{\mu_R} \\ 0 & -(\mathrm{Y}_H + \mu_H) & \frac{\tau_2 B}{\mu_H} & 0 & 0 & 0 & 0 & 0 & 0 & \frac{\tau_1 \lambda_R}{\mu_R} \\ 0 & \mathrm{Y}_H & -(\mathrm{Y}_{1H} + \mathrm{Y}_{2H} + \mu_H + \delta) & 0 & 0 & 0 & 0 & 0 & 0 & 0 \\ 0 & 0 & \mathrm{Y}_{1H} & -(\mathrm{Y}_{3H} + \mu_H + \delta) & 0 & 0 & 0 & 0 & 0 & 0 \\ 0 & 0 & \mathrm{Y}_{2H} & 0 & -(\sigma_H + \mu_H + \delta) & 0 & 0 & 0 & 0 & 0 \\ 0 & 0 & 0 & \mathrm{Y}_{3H} & 0 & -(\sigma_H + \mu_R + \delta) & 0 & 0 & 0 & 0 \\ 0 & 0 & 0 & 0 & \sigma_{1H} & \sigma_H & -\mu_H & 0 & 0 & 0 \\ 0 & 0 & 0 & 0 & 0 & 0 & 0 & -\mu_R & 0 & 0 \\ 0 & 0 & 0 & 0 & 0 & 0 & 0 & 0 & -(\mathrm{Y}_R + \mu_R) & \frac{\tau_3 \lambda_R}{\mu_R} \\ 0 & 0 & 0 & 0 & 0 & 0 & 0 & 0 & \mathrm{Y}_R & -\mu_R \end{pmatrix} \quad (10)$$

And solving the equation

$$\left| J_{E^0} - \lambda \mathrm{I} \right| = 0 \quad (11)$$

$\lambda_1 = -\mu_H < 0$, $\lambda_3 = -\mu_R < 0$, $\lambda_4 = -(\sigma_{1H} + \mu_H + \delta) < 0$, $\lambda_5 = -(\sigma_H + \mu_H + \delta) < 0$,

$\lambda_6 = -(\sigma_H + \mu_H + \delta) < 0$, $\lambda_7 = -\mu_H < 0$, $\lambda_4 = -(\sigma_H + \mu_H + \delta) < 0$,

The remaining eigenvalues are determined from the characteristic equation.

$$A_1\lambda^4 + A_2\lambda^3 + A_3\lambda^2 + A_4\lambda + A_0 = 0 \quad (12)$$

Where

$A_1 = 1$, $A_2 = ((b_9 + b_{10}) + (b_2 + b_3))$,

$A_3 = ((b_2 + b_3)(b_9 + b_{10}) + b_2 b_3 + b_9 b_{10} - \mathrm{Y}_R C_{910} - \mathrm{Y}_H C_{22})$

$A_4 = ((b_2 + b_3)(b_9 + b_{10}) + (b_2 + b_3)(b_9 b_{10}) - (b_2 + b_3)\mathrm{Y}_R C_{910} - b_2 b_3 \mathrm{Y}_R C_{910} - \mathrm{Y}_H C_{22}(b_9 + b_{10}))$

,

$A_0 = ((b_2 b_3)(b_9 b_{10}) + \mathrm{Y}_H C_{22} \mathrm{Y}_R C_{910} - b_2 b_3 \mathrm{Y}_R C_{910} - \mathrm{Y}_H C_{22} b_9 b_{10}$

We can determine that all the roots of the polynomial (12) have negative real parts if and only if the coefficients Ai are positive and the determinant of the matrices meets a specific condition Hi > 0, for i = 1, 2, 3, 4, by using the Routh-Hurwitz criterion. Thus, we can conclude that

$$H = \begin{vmatrix} A_1 & 1 & 0 & 0 \\ A_1 & A_2 & A_3 & 1 \\ 0 & A_0 & A_1 & A_0 \\ 0 & 0 & 0 & A_0 \end{vmatrix} = A_3 \begin{vmatrix} A_2 & A_0 & 0 \\ A_3 & A_1 & 0 \\ 1 & A_2 & A_0 \end{vmatrix} - A_1 \begin{vmatrix} 1 & A_0 & 0 \\ 0 & A_1 & 0 \\ 0 & A_2 & A_0 \end{vmatrix}$$

(13)

$= A_3A_2A_1A_0 - A^2{}_3A^2{}_0 - A_3A^2{}_0 > 0$ If and only If $-(A^2{}_3A^2{}_0 - A_3A^2{}_0) < 0$

Thus, all the eigenvalues of the polynomial (12) have negative real components, indicating that $\lambda_2 < 0, \lambda_3 < 0, \lambda_9 < 0, \lambda_{10} < 0$. All the values $\lambda_i < 0$, for $i = 1.2.,3,...10.$ when

$R_0 < 1$ Thus, the disease-free equilibrium point is locally stable and converges to stability over time.

Global Stability Analysis of the disease – free equilibrium point

A comprehensive investigation into the global stability of the disease-free equilibrium point was carried out using the methodology introduced by Castillo-Chavez, Feng, and Huang in 2002. To ascertain the system's global stability, it was imperative to satisfy two essential conditions. The models (1) were reformulated into the following representation:

$$\frac{dX}{dt} = F(X, Z)$$

$$\frac{dZ}{dt} = G(X, Z), G(X, 0) = 0$$

(14)

X, represented by (SH, RH, SR), stands for the count of individuals in the uninfected population, whereas S denotes those who are infected. The Disease-Free State is indicated

by a specific symbol. To ensure global asymptotic stability, two conditions, H1 and H2, must be satisfied:

H1: The system is globally asymptotically stable for S. H2: There exists a matrix M (with non-negative diagonal elements in matrix C) within a biologically feasible region.

Lemma 1: A point, referred to as K0 = (X0, 0), is termed a stable asymptotic equilibrium point if, in addition to R0< 1, both conditions H1 and H2 are met. The formulation of Theorem 2 is based on the principles established in Lemma 1.

Theorem 2: If R0 < 1, then the equilibrium in which the disease is absent is globally asymptotically stable.

Proof: Consider X = (SH, RH, SR), , and K0 = (X0, 0).

Where $X^0 = (\frac{B}{\mu_H}, 0, \frac{\lambda_R}{\mu_R})$ $\quad X \Rightarrow R^3$

$$\frac{dS_H}{dt} = B\left[1-(Ve\times c)\right]-(\tau_1 \mathrm{I}_{RH} + \tau_2 \mathrm{I}_{HH} + \mu_H)S_H$$

$$\frac{dR_H}{dt} = \sigma_H C_H + \sigma_{1H} U D_H + B(Ve\times c) - \mu_H R_H$$

$$\frac{dS_R}{dt} = \lambda_R - \tau_3 \mathrm{I}_R S_R - \mu_R S_R$$

$$F(X,0) = \begin{pmatrix} B-\mu_H S_H \\ 0 \\ \lambda_R - \mu_R \end{pmatrix}$$

$$X \Rightarrow R^7$$

$$\frac{dE_H}{dt} = (\tau_1 \mathrm{I}_{RH} + \tau_2 \mathrm{I}_{HH})S_H - (\mu_H + \mathrm{Y}_H)E_H$$

$$\frac{\partial \mathrm{I}_H}{\partial t} = \mathrm{Y}_H E_H - (Y_{1H} + Y_{2H} + \mu_H + \delta)\mathrm{I}_H$$

$$\frac{dD_H}{dt} = Y_{1H}\mathrm{I}_H - (Y_{3H} + \mu_H + \delta)D_H$$

$$\frac{dUD_H}{dt} = Y_{2H}\mathrm{I}_H - (\sigma_{1H} + \mu_H + \delta)UD_H$$

$$\frac{dC_H}{dt} = Y_{3H}D_H - (\sigma_H + \mu_H + \delta)C_H$$

$$\frac{dE_R}{dt} = \tau_3 \mathrm{I}_R S_R - (\mathrm{Y}_R + \mu_R)E_R$$

$$\frac{d\mathrm{I}_R}{dt} = \mathrm{Y}_R E_R - \mu_R \mathrm{I}_R$$

$$C = \begin{pmatrix} -(\mathrm{Y}_H + \mu_H) & \tau_2 S_H & 0 & 0 & 0 & 0 & \tau_1 S_H \\ \mathrm{Y}_H & -(\mathrm{Y}_{1H} + \mathrm{Y}_{2H} + \mu_H + \delta) & 0 & 0 & 0 & 0 & 0 \\ \mathrm{Y}_{1H} & -(\mathrm{Y}_{3H} + \mu_H + \delta) & 0 & 0 & 0 & 0 & 0 \\ 0 & \mathrm{Y}_{2H} & 0 & -(\sigma_H + \mu_R + \delta) & 0 & 0 & 0 \\ 0 & 0 & \mathrm{Y}_{3H} & 0 & -(\sigma_H + \mu_R + \delta) & 0 & 0 \\ 0 & 0 & 0 & 0 & 0 & -(\mathrm{Y}_R + \mu_R) & \tau_3 S_R \\ 0 & 0 & 0 & 0 & 0 & \mathrm{Y}_R & -\mu_R \end{pmatrix} \tag{15}$$

$$G(X,Z) = \begin{pmatrix} G_1(X,Z) \\ G_2(X,Z) \\ G_3(X,Z) \\ G_4(X,Z) \\ G_5(X,Z) \\ G_6(X,Z) \\ G_7(X,Z) \end{pmatrix} = \begin{pmatrix} (\tau_1 I_R + \tau_2 I_H)\left(1 - \dfrac{S}{N_H}\right) \\ 0 \\ 0 \\ \tau_1 I_R \left(1 - \dfrac{S}{N_R}\right) \\ 0 \\ 0 \end{pmatrix} \begin{pmatrix} E_H \\ I_H \\ D_H \\ UD_H \\ C_H \\ E_R \\ I_R \end{pmatrix} \tag{16}$$

Since $S_H < N_H$ and $S_R < N_R$ with $G_1, G_2\ G_3, G_4, G_5, G_6,\ G_7 \geq 0$. Therefore, all the two conditions H_1 and H_2 were met, then by lemma (I) above, the disease free equilibrium is globally asymptotically stable when $R_0 < 1.$

RESULTS AND DISCUSSION

We used the values in table 1 to generate the graphical simulation with respect to the model equation (1).

Variables/Parameters	Values	Source
B	0.15	Onuorahet'al (2016)
μ_H	0.0003465	WHO(2016)
γ_H	0.9	Onuorahet'al (2016)
σ	0.6	Onuorahet'al (2016)
τ_1	0.024-0.048	Nakulet'al (2008)
τ_2	0.022-0.27	Nakulet'al (2008)
τ_3	0.12	Assumed
μ_R	0.00641026-0.0038	Mohammed et al. (2015)
γ_R	0.24-0.8	Mohammed et al. (2015)
c	0.8	Assumed
σ_{1H}	0.7	Assumed
ve	0.11	Assumed
δ	70	NCDC (2020)
Λ_R	0.033	Bakareet'al (2019)
γ_{1H}	12	Assumed
γ_{2H}	9	Assumed
γ_{3H}	15	Assumed
S_H	100000	NCDC (2020)
S_R	5000	Bakareet'al (2019)
E_H	1706	NCDC (2020)
I_H	109	NCDC (2020)

C_H	476	NCDC (2020)
D_H	76	NCDC (2020)
UD_H	0	NCDC (2020)
R_H	1310	NCDC (2020)
E_R	23	Assumed
I_R	55	Assumed

In our numerical simulation of the deterministic model, we assessed the influence of various parameters on different population groups, including susceptible humans, susceptible rodents, total infectious humans, and total infectious rodents, using the initial population values provided in Table 1. Parameters were systematically adjusted at different time intervals to gain insight into their effects on population dynamics.

For instance, as shown in Figure 1a, we observed that the introduction of a vaccine had a significant impact on the population of susceptible humans. As vaccine effectiveness increased, the number of susceptible individuals decreased, suggesting that the eradication of Lassa fever could be achievable if all susceptible humans were safeguarded by long-term immunity-conferring vaccines, as indicated in our model.

Furthermore, Figure 1b demonstrated that the natural death rate had a considerable effect on the susceptible human population, leading to population variations across different parameter values. Similarly, Figure 1c highlighted the substantial influence of the transmission parameter on the susceptible human population, with increased contacts between rodents and humans resulting in higher Lassa fever transmission and reduced susceptible human populations.

However, Figure 1d presented an unexpected finding: the parameter representing contact between infected and susceptible humans had a minimal effect on the susceptible human population. This contradicted the typical mode of disease transmission through contact with infected individuals, suggesting the importance of other factors in disease transmission.

Moving on to Figure 2a, we explored the impact of the progression parameter from exposed to infected humans on the total infectious human population, observing a decrease in total infectious individuals as this parameter increased, especially during later time intervals. Figure 2b indicated that vaccination significantly affected the total infectious

human population, with increased vaccination leading to a decline in total infectious individuals.

In Figure 2c, the natural death parameter exhibited a substantial impact on the total infectious human population. An increase in this parameter resulted in a decrease in the total infected and infectious population, eventually stabilizing after a certain time interval. Figure 2d illustrated the significant effect of the transmission probability from rodents to humans on the total infectious human population, with an increase in this parameter leading to an increase in infectious individuals.

In a similar fashion, Figure 2e revealed that the transmission probability from one human to another exerted a noteworthy impact on the overall infectious population, with higher transmission rates resulting in an increase in the total infectious population, which eventually stabilized. However, Figure 2f and Figure 2g indicated that the progression parameters from infected to detected and undetected human populations had negligible effects on the total infectious human population.

Figure 2h presented another unexpected result: the parameter representing Lassa fever-induced deaths had an insignificant effect on the total infectious human population. This finding was surprising given the severity of Lassa fever symptoms and the potential for death within 14 days. Nonetheless, the population remained stable over time intervals 6-10.

Furthermore, we investigated the influence of these parameters on the detected human population, which includes individuals identified as Lassa fever cases through laboratory diagnosis. For instance, Figure 3a revealed that the transmission parameter from rodents to humans influenced the detected human population, with higher transmission rates leading to larger detected populations. Similarly, Figure 3b indicated a similar trend, with the transmission parameter from human to human affecting the detected population.

In Figure 3c, the death parameter due to Lassa fever influenced the detected human population, resulting in a decrease in the detected population as Lassa fever-induced deaths increased. Figure 3d highlighted the positive impact of vaccination on the detected human population.

Figure 3e showed that the progression parameter 'Y2H' had an effect on the detected human population, causing a decrease as this parameter increased, especially for smaller parameter values. In Figure 3f, the progression parameter from exposed to infected human populations influenced the detected population, leading to an increase with higher values of

this parameter. Finally, Figure 3g indicated that the natural death rate had a negative influence on the detected human population, with higher death rates resulting in decreased detected populations.

Subsequently, Figures 4a to 4h explored the effects of parameters on the population of undetected humans, individuals who may have had contact with infected persons but have not yet been identified as Lassa fever cases. For example, Figure 4a demonstrated that the natural human death rate had a significant effect on the undetected human population, with higher death rates leading to population decreases.

In Figure 4b, the progression rate parameter from rodents to humans influenced the undetected population, with increased parameter values resulting in decreased undetected populations. Figure 4c showed that the progression parameter from human to human had a positive effect on the undetected population, leading to increased undetected populations with higher values of this parameter. Figures 4d and 4e illustrated the influence of vaccination and progression parameters on the undetected population.

However, Figures 4f and 4g demonstrated that the progression parameters from infected to detected and undetected human populations had limited effects on the undetected population, leading to insignificant population changes. Finally, in Figure 4h, the progression parameter from undetected to recovered human populations had an insignificant effect on the undetected population, with the population remaining relatively stable regardless of changes in this parameter.

Lastly, in Figures 5a to 5h, we investigated the effects of parameters on the Isolation Human population, introduced to control the spread of Lassa fever. For instance, in Figure 5a, the progression parameter from detected to isolation human had a limited impact on the Isolation Human population, with minimal changes observed as the parameter value increased, which was unexpected given the typical isolation of infected individuals for treatment.

In Figure 5b, the transmission parameter from rodents to humans significantly affected the Isolation Human population, with increased transmission rates resulting in larger Isolation Human populations, potentially aiding in disease control. Similarly, in Figure 5c, the death parameter due to Lassa fever influenced the Isolation Human population, with increased deaths leading to population decreases.

In Figure 5d, the natural death parameter had a substantial effect on the Isolation Human population, with a noticeable decrease as the parameter value increased, which could impact the effectiveness of isolation strategies. In Figure 5e, the transmission parameter from rodent to rodent had a significant effect on the susceptible rodent population, with increased reproduction among rodents leading to a decrease in the susceptible population, highlighting the importance of controlling rodent population growth.

Lastly, Figure 6b indicated that the parameter representing contact between infected and susceptible rodents had a substantial impact on the susceptible rodent population, with increased interactions resulting in more rodents becoming infected and reducing the susceptible population.

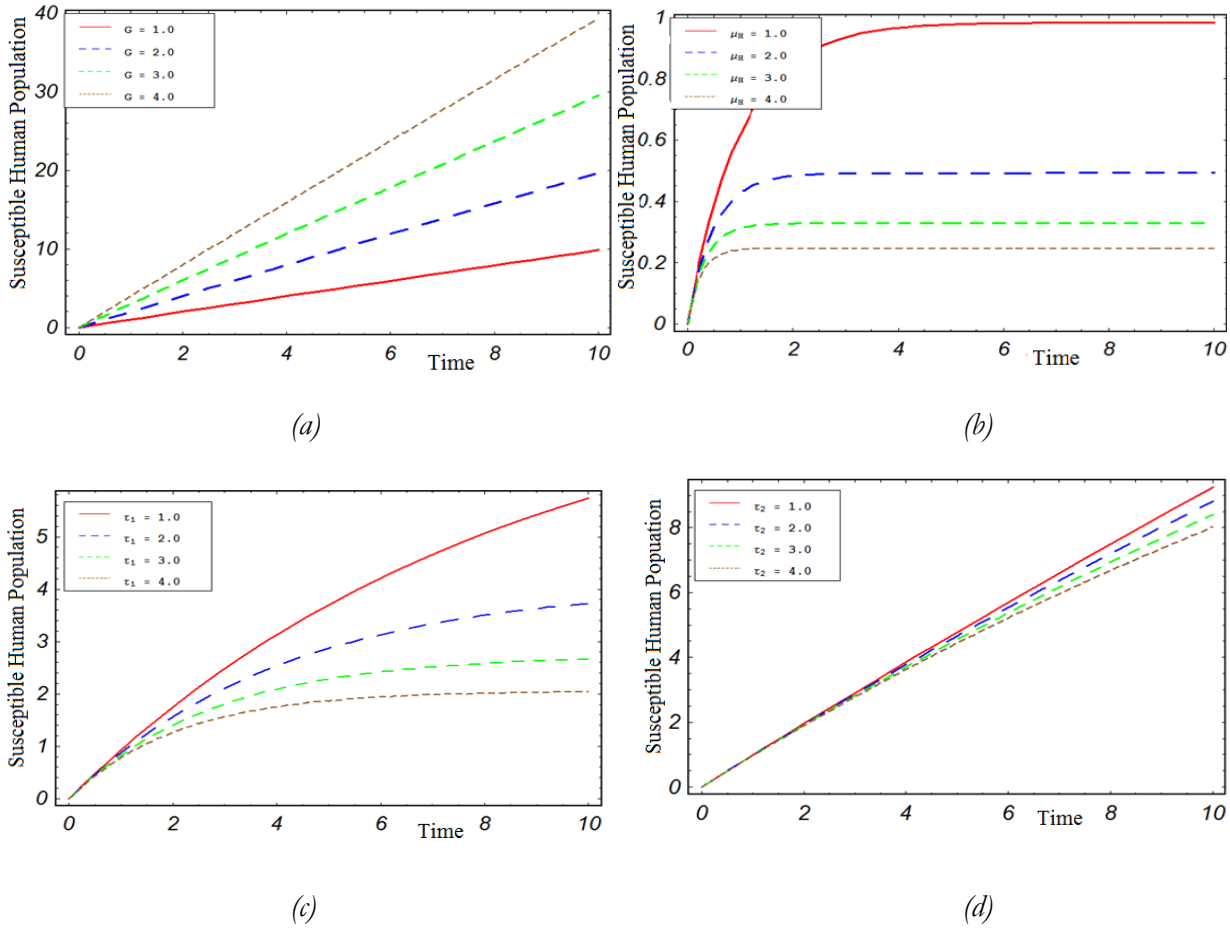


Figure 1: Susceptible Human Population against time showing the Influence of each parameter at different values (1.0; 2.0; 3.0, 4.0).

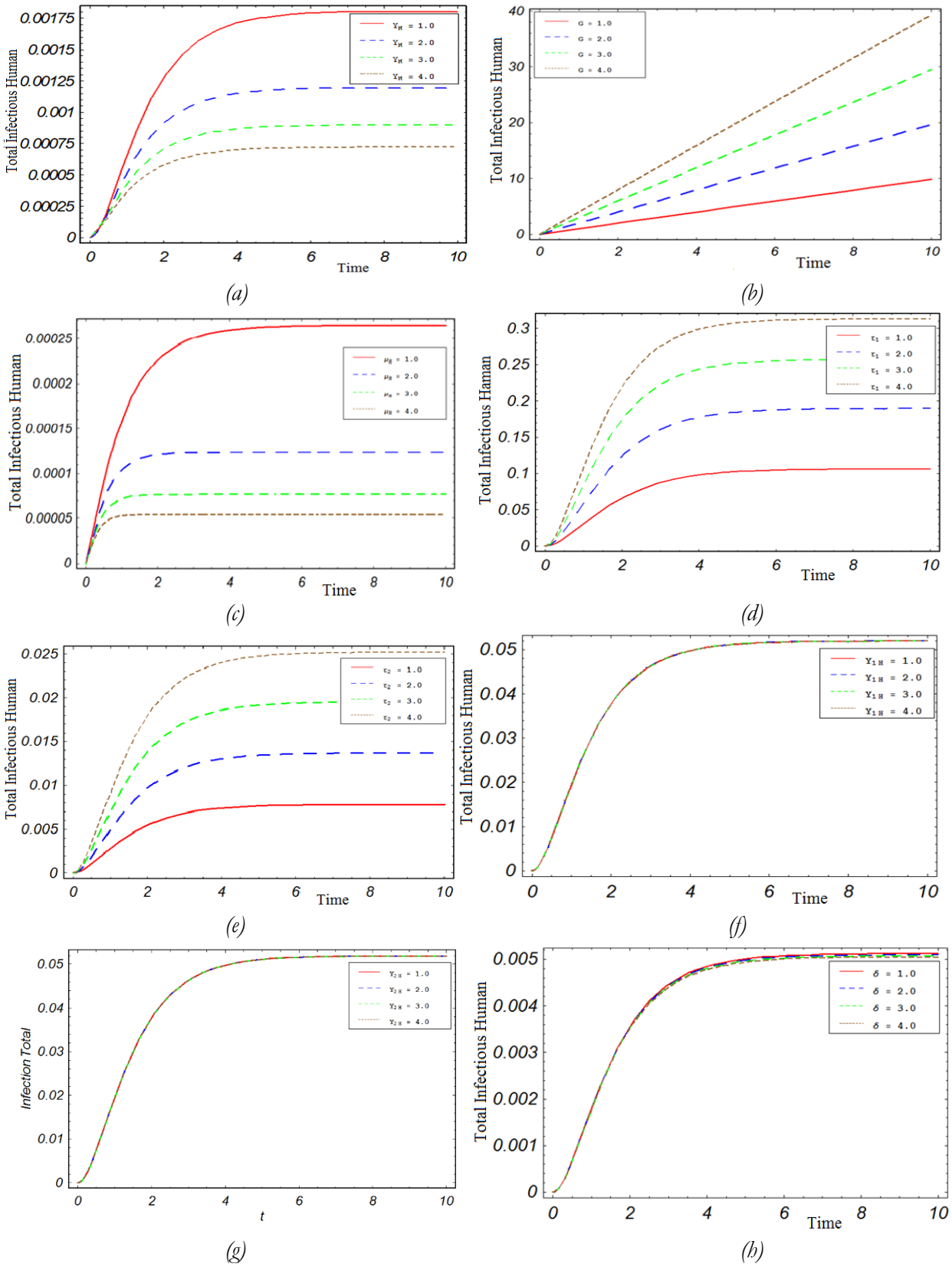


Figure 2: Total infection human against time showing the Influence of each parameter on the populations at different values (1.0, 2.0, 3.0, and 4.0).

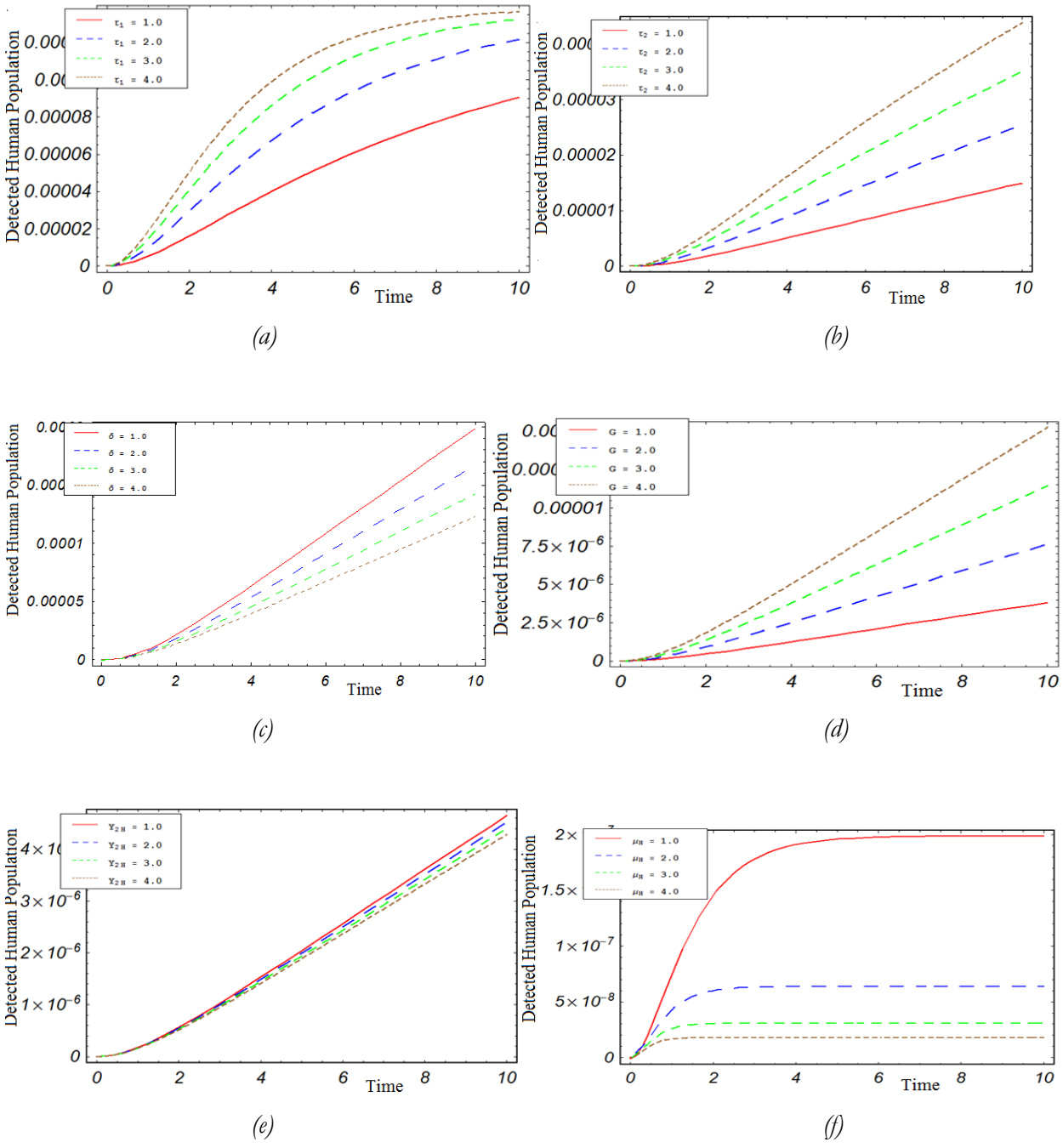


Figure 3: Detected Human Population against time showing the Influence of each parameter on the population (1.0; 2.0; 3.0, 4.0).

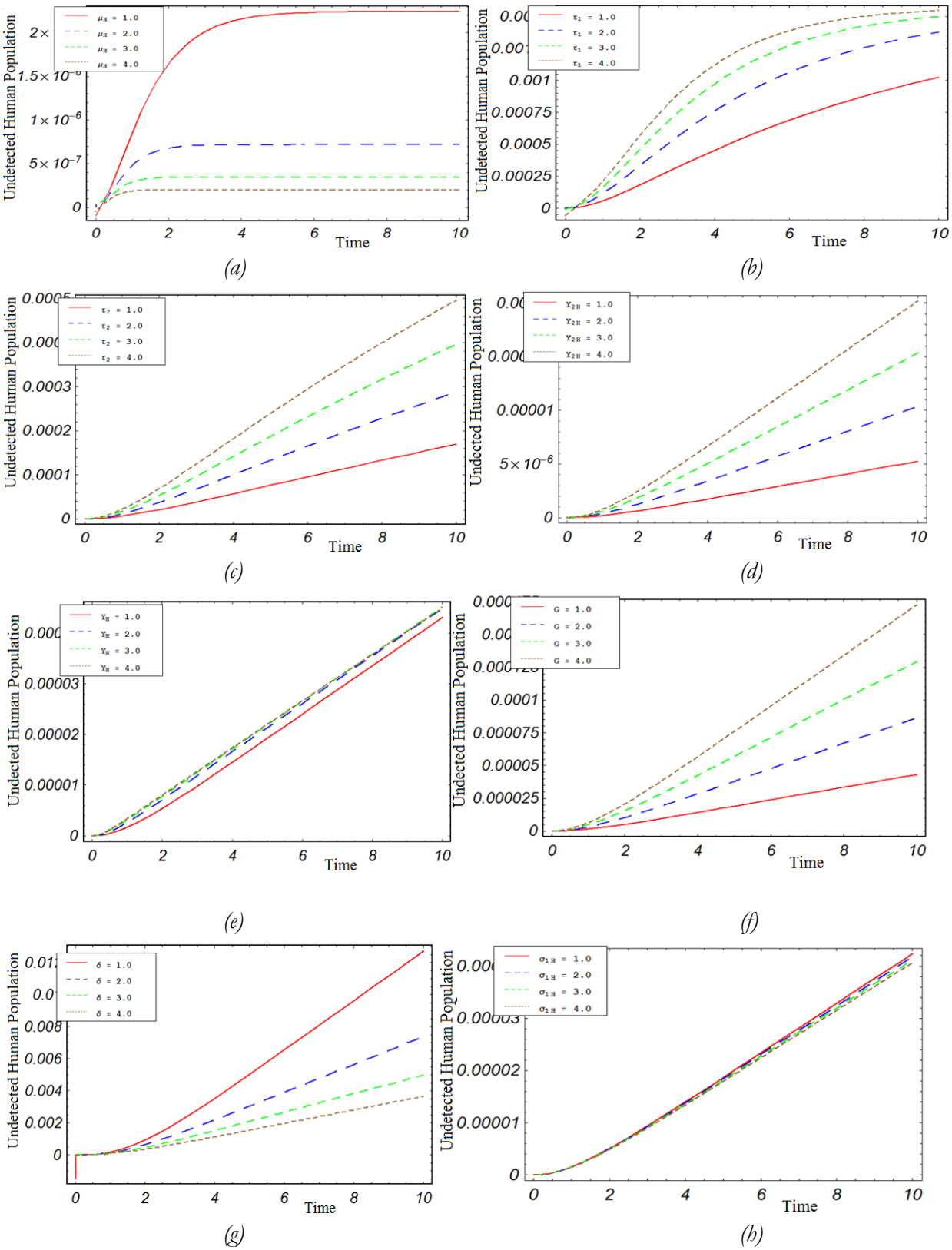


Figure 4: Undetected Human Population against time showing the Influence of each parameter on the population at different values (1.0; 2.0; 3.0, 4.0).

.

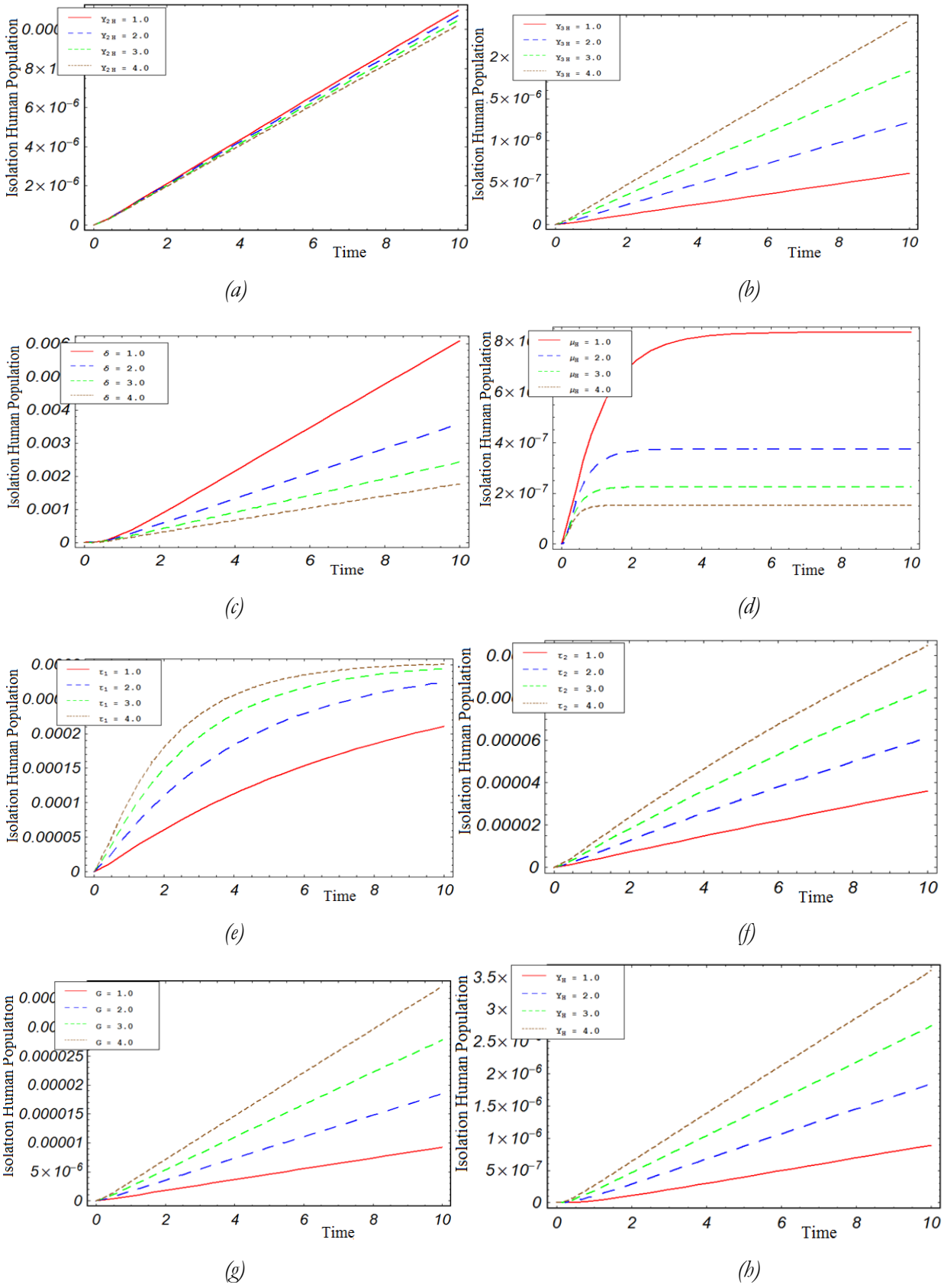


Figure 5: Isolated Human Population against time showing the Influence of each parameter on the population at different values: (1.0, 2.0, 3.0 and 4.0).

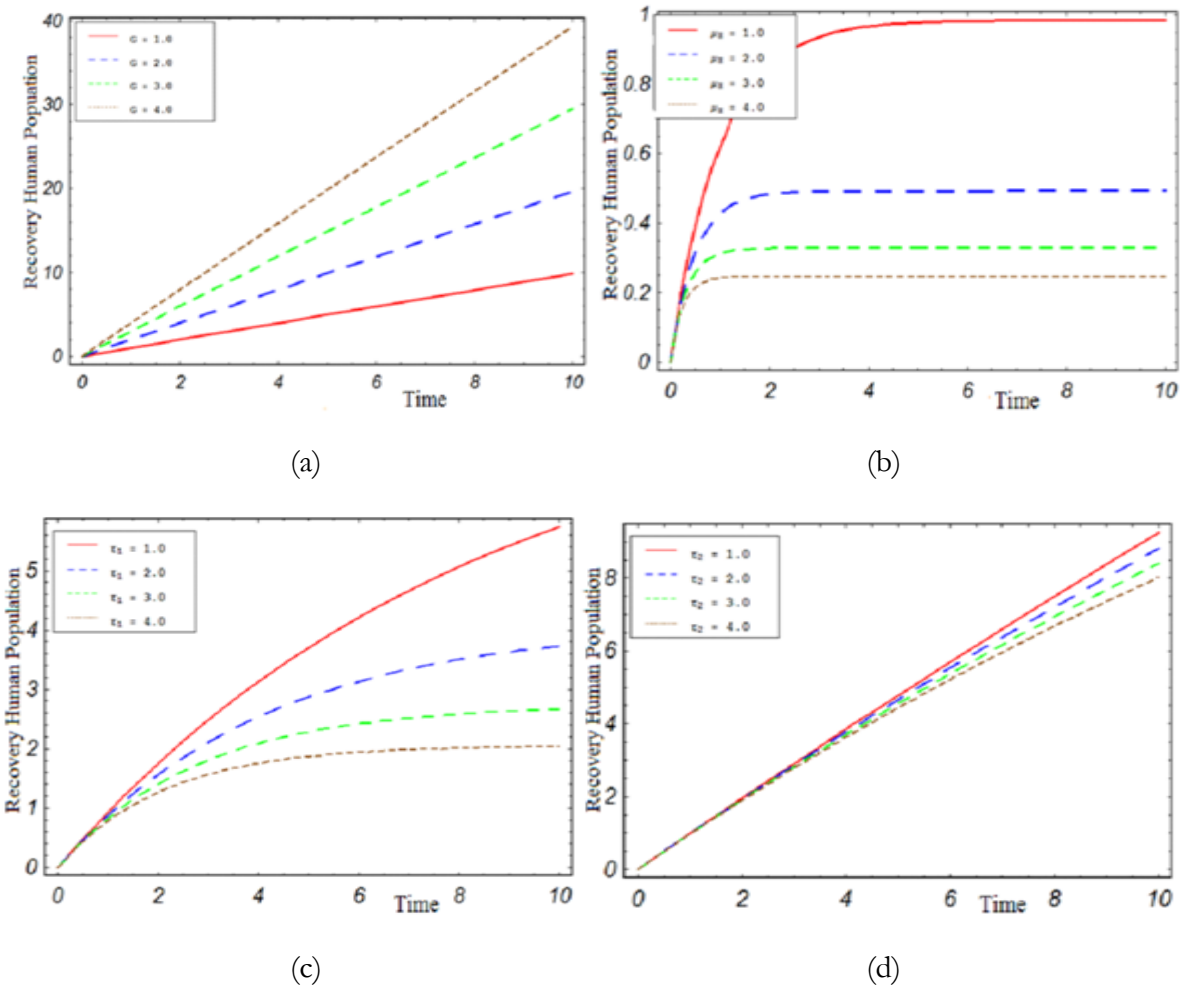
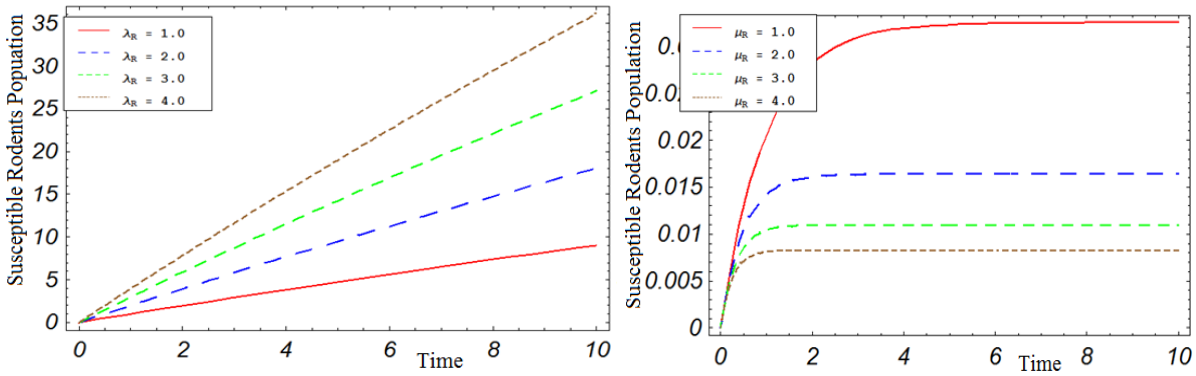
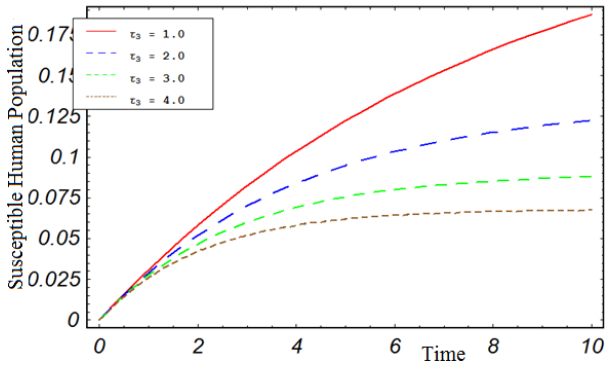


Figure 6:Recovery Human Population against time showing the Influence of each parameter on the population at different values: (1.0, 2.0, 3.0, 4.0*)*

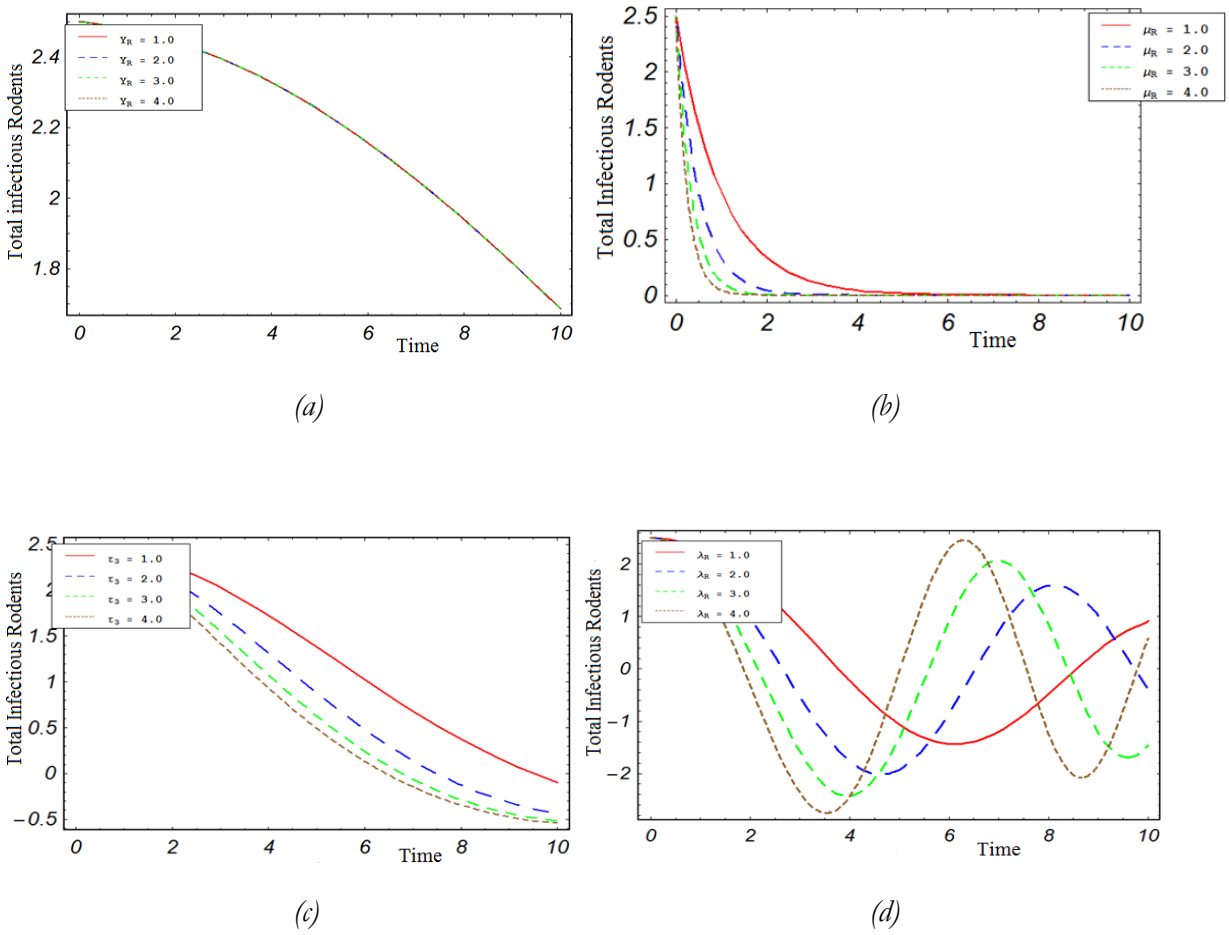


(a) *(b)*



(c)

Figure 7: Susceptible Rodents population against time showing the Influence of each parameter on the population at different values (1.0, 2.0, 3.0, 4.0).



(a) *(b)*

(c) *(d)*

Figure 8: Total infectious Rodents against time showing the influence of each parameter on the population at different values $(1.0, 2.0, 3.0, 4.0)$.

CONCLUSION

Our exploration of Lassa fever models was aimed at acquiring a more profound comprehension of its transmission dynamics. We employed nonlinear ordinary differential equations to portray the system's behavior while rigorously ensuring that it remains within defined, positive, and bounded limits. The stability of solutions within this prescribed region remained unaltered, thereby affirming the mathematical and epidemiological validity of our methodology. Our investigation encompassed the calculation of the basic reproduction number using the next-generation matrix technique, as well as an extensive stability analysis concerning the disease-free equilibrium within the model. Our scrutiny unveiled that the disease-free equilibrium attains local stability when the basic reproduction number falls below one ($R_0 < 1$) and becomes unstable when R_0 exceeds one ($R_0 > 1$).

Furthermore, we conducted numerical simulations employing Mathematica 5.2, yielding outcomes that concurred with our analytical findings. A noteworthy observation emerged: the vaccination of individuals wielded a substantial influence on curtailing the propagation of Lassa fever. This implies that the transmission of Lassa fever can be effectively arrested through the vaccination of a substantial portion of the population.

REFRENCES

1. Richmond, J. K. and Baglole D. J. (2003). Lassa fever: epidemiology, clinical features, and social consequences. BMJ, 327: 1271–5.
2. Gibb, R., Moses, L. M., Redding, D. W., and Jones, K. E. (2017). Understanding the cryptic nature of Lassa fever in West Africa. Pathog Glob Health, 111(6):276–88.
3. A. R. Akhmetzhanov, Y. Asai and H. Nishiura, (2019). Quantifying the seasonal drivers of transmission for Lassa fever 364 in Nigeria, Phil. Trans. R. Soc. -B, 374, 2018.
4. E. Fichet-Calvet and D. J. Rogers, (2009). Risk Maps of Lassa fever in west Africa, PLoSNegl. Trop. Dis., 3.
5. Katherine J. Siddle, Philomena Eromon, Kayla G. Barnes, Samar Mehta. (2018). Genomic Analysis of Lassa Virus during an Increase in Cases in Nigeria in 2018. The New England Journal of Medicine: **DOI: 10.1056/NEJMoa1804498**
6. Kolawole S, Dimitrios G, Connie S, Melanie S and Nadia T. (2019). A review of Lassa fever vaccine candidates. Current Opinion in Virology 2019, 37:105–111.
7. D. E. Carey, G. E. Kemp, H. A. White, et al., (1972). Lassa fever epidemiological aspects of the 1970 epidemic, Jos, 380 Nigeria, Trans. R. Soc. Trop. Med. Hyg., 66, 402-408.
8. G. Chowell, L. Sattenspiel, S. Bansal and C. Viboud, (2016). Mathematical models to characterize early epidemic growth: A review, Phy. Life Rev., 18, 66-97.
9. S. P. Fisher-Hoch, O. Tomori, A. Nasidi, et al., (1995). Review of cases of nosocomial Lassa fever in Nigeria: the high price of poor medical practice, Brit. Med. J., 311, 857.
10. E. L. Hamblion, P. Raftery, A. Wendland, et al., (2018). The challenges of detecting and responding to a Lassa fever outbreak in an Ebola-affected setting, Int. J. Infect. Dis., 66, 65-73.
11. A. H. Demby, A. Inapogui, K. Kargbo, J. Koninga, K. Kourouma, et al., (2004). Lassa Fever in Guinea: II. Distribution and Prevalence of Lassa Virus Infection in Small Mammals, Vector Borne Zoonotic Dis., 4.
12. A. M. Saez, M. C. Haidara, A. Camara, F. Kourouma, M. Sage, and N. Magassouba, et al., (2018). Rodent control to fight Lassa fever: evaluation and lessons learned from a 4-year study in Upper Guinea, PLoSNegl. Trop. Dis., 12.

13. Bawa M., Abdulrahman S., Jimoh O.R., Adabara N.U. (2014). Stability Analysis of the Disease-Free Equilibrium State for Lassa Fever Disease. Journal of Science Technology, Mathematics and Education, Vol 9(2).
14. Mohammed B.A., Umar C.D., Mamman M. (2015). Sensitivity Analysis in a Lassa Fever Deterministic Mathematical Model. Citation: 1660, 050050 (2015); doi: 10.1063/1.4915683.Published by the American Institute of Physics.
15. Onuorah, M. O, Akinwande N.I., Nasir M.O and Ojo M.S. (2016) Sensitivity Analysis of Lassa Fever Model : International Journal of Mathematics and Statistics Studies Vol.4, No.1, pp.30-49, February 2016 _Published by European Centre for Research Training and Development UK (www.eajournals.org)
16. Joachim, M., Benny, B., Fodé, K., Jatta, B., Toni, R., Stephan, G., N'Faly, M., Herwig, L. & Elisabeth, F.C. (2019) Evaluation of rodent control to fight Lassa fever based on field data and mathematical modelling, Emerging Microbes & Infections, 8:1, 640-649, DOI: 10.1080/22221751.2019.1605846
17. Bakare, E.A., Are, E.B., Abolarin, O.E.,Osanyinlusi, S.A., NgwuBenitho, UbakaObiaderi, N. (2019) Mathematical Modelling and Analysis of Transmission Dynamics of Lassa fever
18. Mary, A. (2019) Mathematical Modeling and Stability Analyses of Lassa Fever Disease with the Introduction of the Carrier Compartment. **Article** · June 2019 DOI: 10.7176/MTM; https://www.researchgate.net/publication/334250540
19. Nwasuka S.C., Nwachukwu I.E. and Nwachukwu P.C. (2019). Mathematical Model of the Transmission Dynamics of Lassa Fever with Separation of Infected Individual and Treatment as Control Measures. Journal of Advances in Mathematics and Computer Science. 32(6): 1-15.
20. Josephine D., Kamalini L., Kathryn G. (2019). Routine and pulse vaccination for Lassa virus could reduce high levels of endemic disease: A mathematical modelling study. Vaccine 37, 3451–3456
21. Salihu S. Musa, Shi Zhao, Daozhou G., Qianying Lin, Gerardo Chowel, Daihai He1. (2019). Mechanistic modelling of the large-scale Lassa fever epidemics in Nigeria from 2016 to 2019. Journal of Theoretical Biology (2020), doi: https://doi.org/10.1016/j.jtbi.2020.110209.
22. Nwasuka, S. C., Nwachukwu, I. E. and Nwachukwu, P.C. (2019) Mathematical Model of the Transmission Dynamics of Lassa Fever with Separation of Infected Individual and Treatment as Control Measures: Journal of Advances in Mathematics and Computer Science; 32(6): 1-15, 2019; Article no.JAMCS.48982; *ISSN: 2456-9968*
23. Xinhong, Z.&Hao, P. (2020) Stationary distribution of a stochastic cholera epidemic model with vaccination under regime switching; Applied Mathematics LettersVolume 102, April 2020, 106095; https://doi.org/10.1016/j.aml.2019.106095
24. Wang, Y. & Cao, J., (2014) Global dynamics of a network epidemic model for waterborne diseases spread, Appl. Math. Comput. 237 (2014) 474–488.
25. Wang, Y. & Cao, J., (2015) Global stability of general cholera models with nonlinear incidence and removal rates: J. Frankl. Inst. 352 (2015) 2464–2485